Progress with High-Field Superconducting Magnets for High-Energy Colliders

G. Apollinari, S. Prestemon and A.V. Zlobin

***Abstract* - One of the possible next steps for HEP research relies on a high-energy hadron or muon collider. Energy of a circular collider is limited by the strength of bending dipoles and its maximum luminosity is determined by the strength of final focus quadrupoles. That is why there has been a permanent interest to higher field and higher gradient accelerator magnets from the high energy physics and accelerator communities. The maximum field of NbTi magnets used in all present high-energy machines including LHC is limited by ~10 T at 1.9 K. The fields above 10 T became possible using the Nb_3Sn superconductor. Nb_3Sn accelerator magnets can provide operating fields up to ~15 T and significantly increase the coil temperature margin. Accelerator magnets with operating field above 15 T require high-temperature superconductors. This paper discusses the status and main results of the Nb_3Sn accelerator magnet R&D and the work towards the 20 T class magnets.**

***Index Terms*— Accelerator magnets, dipole and quadrupole coils, magnet R&D.**

I. Introduction

The adoption of superconducting (SC) magnets has been a true success story for the high-energy physics (HEP) community, and there have been a number of important spin-off applications of this technology in the field of health care (such as MRI). From the pioneering work performed in the early 1970s at Brookhaven National Laboratory (BNL) and Rutherford Accelerator Laboratory (RAL) through the construction and 25-year operation of the Tevatron at Fermi National Accelerator Laboratory (FNAL), the first large accelerator based on SC magnets, to the latest and greatest achievements of the Large Hadron Collider (LHC) at the European Organization for Nuclear Research (CERN) 40 years later, the use of SC magnets for HEP has enabled discoveries ranging from the top quark in 1994 [1] to the Higgs particle in 2012 [2], with multiple additional measurements that have shaped and confirmed our understanding of the Standard Model. The successful performance of the LHC and the recent discovery of the Higgs particle, which earned a Nobel Prize for François Englert and Peter W. Higgs in 2013, have been widely covered in the literature and the popular press. Since the 1970s, the workhorse for the SC magnet field has been NbTi superconducting alloy, thanks to both the ductility of the material and the impetus provided to the manufacturing industries by the construction of the Tevatron. The NbTi accelerator magnets in the LHC are reaching their practical operation limit of ~8 T with the appropriate operational margin.

A possible next step for fundamental HEP research relies on a hadron collider (HC) or a muon collider (MC) operating at higher energies. Several studies for post-LHC proton colliders have been and are now being conducted; these include the Very Large Hadron Collider (VLHC) [3] and Muon Collider (MC) [4] studies in the United States and the recently begun Future Circular Collider (FCC) and SppC studies in the European Union and China, respectively (https://espace2013.cern.ch/fcc/Pages/default.aspx). This review focuses on a discussion of the results obtained so far, as well as plans for future research and development (R&D) on higher-field magnets for these facilities.

II. HF SC Accelerator Magnets - Performance Parameters and Design Features

Two events placed colliders at the forefront of physics investigations. The first was the introduction of the synchrotron acceleration scheme in the 1940s and 1950s [5], and the second was the development of colliders with the AdA and VEP-1 accelerators for lepton machines in the 1960s, followed by the invention of stochastic cooling [6] with the Super Proton Synchrotron for hadron machines in the 1980s. Whereas e^+e^- circular colliders are limited by synchrotron radiation and, therefore, by the strength of the magnetic field encountered by the circulating electron beams, the same is true for hadron and muon colliders only at much higher energies than those achieved so far. For this reason, ever-stronger magnetic fields have been a basic goal in accelerator applications.

The energy E (in GeV) of particles in a circular accelerator is linked to the strength of bending dipole magnets B (in Tesla) and machine radius r (in meters) by the basic relation:

$$E \approx 0.3rB.$$

Thus, a higher field is the most efficient way to achieve higher-energy in machines. In addition to particle bending in a circular machine, magnets are also used both to control the beam in the transverse plane by means of focusing and defocusing quadrupoles and to provide the final focus (FF) for the intersecting beam just before collisions in the experimental hall.

In particle interactions, the rate of events observed is related to the event cross section by the formula:

$$N_{exp} = \sigma_{exp} \cdot \int L(t)dt$$

where $L(t)$ is the instant luminosity. For beams with n_1 and n_2 particles colliding at a frequency of f_{rev}:

$$L = \frac{n_1 n_2 f_{rev}}{4 \beta^* \varepsilon}$$

where ε_n is the normalized transverse emittance and β^* is the betatron function at the interaction point. To maximize L, low β^* has to be achieved in the collision region, which is

Operated by Fermi Research Alliance, LLC under Contract No. De-AC02-07CH11359 with the United States Department of Energy.

determined by the optics of the machine and is proportional to the gradient of the quadrupoles closest to the interaction point.

Field quality and its reproducibility from magnet to magnet are also key parameters for accelerator magnets because in a synchrotron the beam circulates through the machine up to 10^9 times, and any small field imperfection can be magnified by huge factors. Typically, these imperfections have to be kept at the level of 0.01% with respect to the main field component. Other important parameters for magnet design include the Lorentz force and the energy stored in a magnet. The Lorentz forces cause coil deformations and, thus, degrade the field quality and may also lead to a quench. The value of stored energy drives the magnet parameters during a quench. It is necessary to distribute the stored energy in the coil, ensuring that nowhere in the coil do the temperature, thermal stresses, and voltages exceed the allowable values. Both the Lorentz forces and the stored energy are proportional to the size of the magnet bore. Therefore, high-field accelerator magnets tend to have the minimum practical aperture for beam transmission.

Several large accelerators worldwide are equipped with SC magnets. These include the Proton–Antiproton Collider (Tevatron, 1983–2011) at FNAL (United States), Hadron Elektron Ring Anlage (HERA, 1991–2007) at Deutsches Elektronen-Synchroton (DESY, Germany), Relativistic Heavy Ion Collider (RHIC, since 2000) at Brookhaven National Laboratory (BNL, United States), and LHC (since 2008) at CERN (France and Switzerland). Figure 1 shows the magnet main parameters and cryostat cross sections. All these accelerator magnets use high-current Rutherford cables with NbTi composite strands, which have the best combination of mechanical, electrical, and thermal properties for magnet fabrication and operation.

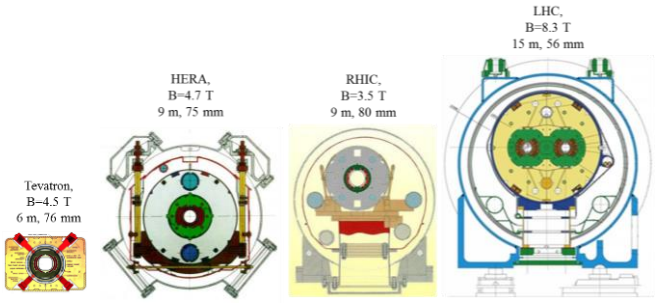

Fig. 1. The accelerator dipoles with cryostats.

The Tevatron was the first SC accelerator in the world and the highest-energy HC until its shutdown in 2011. The Tevatron collider ring has a circumference of ~6.9 km and consists of 774 dipoles and 240 quadrupoles, as well as more than 200 corrector spool pieces. The success of the Tevatron was based on the adoption of the Rutherford cable, the use of two-layer saddle-type coils, the development of a precise collaring system for coil prestress and support, and the use of protection heaters to accelerate the normal zone propagation in the coil during a quench [7]. Tevatron magnets employed a compact cryostat design with a warm yoke.

In the 1980s, DESY began construction of HERA, an e^-p collider. HERA consists of a 30 GeV electron storage ring (SR) with conventional electromagnets and an 820 GeV proton SR. The 820 GeV ring has a circumference of ~6.3 km and consists of 422 main dipoles and ~225 main quadrupoles, along with approximately the same number of SC correcting elements. HERA dipoles, designed to produce 4.7 T at 4.6 K, later operated at 5.5 T by cooling below 4 K. The HERA project was the first to adopt a magnet design with aluminum collars and cold iron and pioneered the industrial manufacturing of 9-m-long magnets [8].

In the 1990s, RHIC was built at BNL. Its ion beams were guided by low-cost dipole magnets of 3.5 T. RHIC consists of two separate SC storage rings, each ~3.8 km in circumference, which intersect in six points. Each ring consists of ~1,740 SC magnets, including 264 arc dipoles and 276 arc quadrupoles. The relatively low operating field allows the use of a single-layer saddle-type coil design in the arc magnets. The coils are surrounded by thick plastic spacers, preloaded and supported by a cold iron yoke. The magnet cold mass is installed inside a vacuum vessel by use of special support posts. Several improvements in the design included the careful determination of the magnetic field in the presence of significant contributions from the iron yoke and the high-quality SC strand and wide Rutherford cable [9].

The LHC is the largest proton collider in the world, with an SC ring circumference of ~27 km. It is located in an underground tunnel at a depth of ~100 m. The ring is filled with 1,276 SC dipoles and ~425 quadrupoles. The dipole and quadrupole design is based on two-layer saddle-type coils preloaded with thick stainless-steel collar laminations and supported by a cold iron yoke. The LHC dipoles use for the first time a two-in-one design concept in which two apertures with opposite-field directions are placed inside a common collar and iron yoke. The LHC's magnets are cooled by superfluid helium at 1.9 K to boost the NbTi performance and utilize the superfluid helium's high thermal conductivity [10].

III. Strands and Cables for HF SC Magnets

In order to increase the magnetic field in accelerator magnets above the level of LHC NbTi magnets, superconductors with higher critical parameters are needed. Among the many known high-field superconductors, at present only Nb_3Sn, Nb_3Al, BSCCO ($Bi_2Sr_2CaCu_2O_8$ or $Bi_2Sr_2Ca_2Cu_3O_{10}$), and REBCO ($REBa_2Cu_3O_7$) [11]–[13] can be used to achieve magnetic fields above 10 T. These superconductors are industrially produced in the form of composite materials in the long lengths (~1 km) required for accelerator magnets. Table 1 provides the critical temperature $T_c(0)$ and the upper critical field $B_{c2}(0)$ for each of these superconductors (see http://www.superconductors.org). The intermetallic composites Nb_3Sn and Nb_3Al are low-temperature superconductors (LTSs), and the metal-oxide ceramics BSCCO and REBCO represent high-temperature superconductors (HTSs).

Table 1. Properties of technical superconductors.

SC material	$T_c(0)$, K	$B_{c2}(0)$, T
Nb_3Sn	18	23*/28
Nb_3Al	18	30*/32
Bi-2212	91	>100
Y-123	92	>100

*data at 4.2 K

A. Strands

The most promising Nb_3Sn composite wires for high-field magnets are based on the internal tin (IT) and powder-in-tube (PIT) processes. In the IT process, niobium filaments and tin rods are assembled in a copper matrix surrounded by a thin niobium or tantalum diffusion barrier to prevent tin leaks into the high-purity copper matrix. This process provides the highest critical current density (J_c), thanks to the optimal amount of tin, but limits the minimal subelement size achievable in the final wire. In the PIT process, thick-walled niobium tubes are filled with fine $NbSn_2$ powder and stacked in a high-purity copper matrix. This method allows an optimal combination of small filament size (<50 μm) and J_c, comparable to those of the IT process. However, the PIT wire cost is a factor of two to three higher than the IT wire cost. In both methods, the Nb_3Sn phase with an optimal pinning structure is formed during a final heat treatment at ~650–700ºC for 50–100 h.

Nb_3Al composite wires are made by stacking Nb-25%Al filaments into a tantalum or niobium matrix, then extruding the assembly down to the required size. The SC Nb_3Al phase is formed by the rapid-heating-quenching transformation (RHQT) process, in which the Nb-Al multifilamentary wire is rapidly heated to ~1,900°C, then quenched into a bath with liquid gallium at ~50°C. A copper stabilizer is added via an ion- or electroplating process. An optimal pinning structure is created during a final heat treatment at 800ºC for 10–15 h. Figure 2 shows typical cross sections of Nb_3Sn wires prepared through the IT and PIT processes and Nb_3Al wires with a niobium and tantalum matrix prepared using the RHQT process.

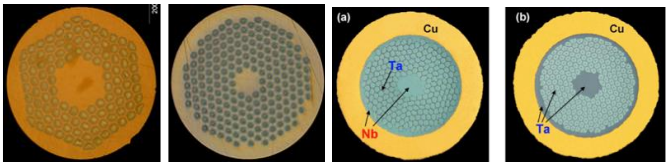

Fig. 2. Nb_3Sn and Nb_3Al composite wires: (a) Nb_3Sn internal tin restack rod process (RRP) (OST, United States); (b) Nb_3Sn powder-in-tube process (Bruker EAS); (c,d) Nb_3Al (NIMS, Japan). Courtesy of J. Parrell (OST), M. Thoener (Bruker EAS), and A. Kikuchi (NIMS).

$Bi_2Sr_2CaCu_2O_8$ (Bi-2212) belongs to the first HTS generation (G1) and is produced using the PIT method. The Ag tubes, filled with a calcined oxide and carbonate powder precursor, are assembled in an Ag matrix and drawn to a final size. Bi-2212 wires require a multistage final heat treatment at very uniform high temperatures with T_{max} up to 900ºC.

$REBa_2Cu_3O_7$ (REBCO), where RE refers to a rare earth element, represents the second generation (G2) coated superconductors. The most known is YBCO composite with chemical composition $YBa_2Cu_3O_{7-x}$ (Y-123). YBCO composite has a complicate architecture and is available only as a tape. Long 4-12 mm wide YBCO tapes are produced using the Ion-Beam-Assisted Deposition (IBAD) method or the Rolling-Assisted Bi-axially Textured Substrate (RABiTS) method. No final heat treatment of the ReBCO tape is needed.

The cross-sections of a Bi-2212 multifilament wire and a YBCO tape are shown in Fig. 3.

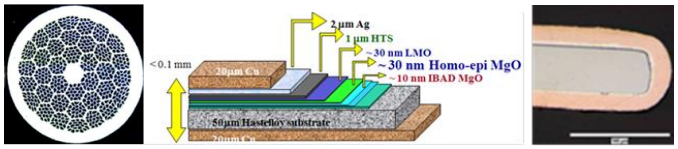

Fig. 3. Bi-2212 wire by OST (left) and YBCO tape by SuperPower, Inc. (center and right).

All SC materials in Table 1 are brittle. The most sensitive to axial and transverse load is Bi-2212 and the least are Nb_3Al and YBCO. Taking into account brittleness of Nb_3Sn, Nb_3Al and Bi-2212, which need final reaction heat treatment, the Wind-and-React (W&R) method is used for small coils with complicated conductor bending. The React-and-Wind (R&W) method is used for large coils with large bending radii.

Engineering current density J_E is the primary parameter for superconducting wires to be used in accelerator magnets. The J_E, defined as the critical current density J_c per total conductor cross-section, depends on the superconductor microstructure and superconductor fraction in the composite cross-section. Figure 4 shows the J_E vs. field B at 4.2 K for the practical high-field HTS (http://fs.magnet.fsu.edu/~lee/plot/plot.htm). Unlike the other three superconducting composites, G2 coated conductors have highly anisotropic J_c and B_{c2} due to the high aspect ratio of the cross-section.

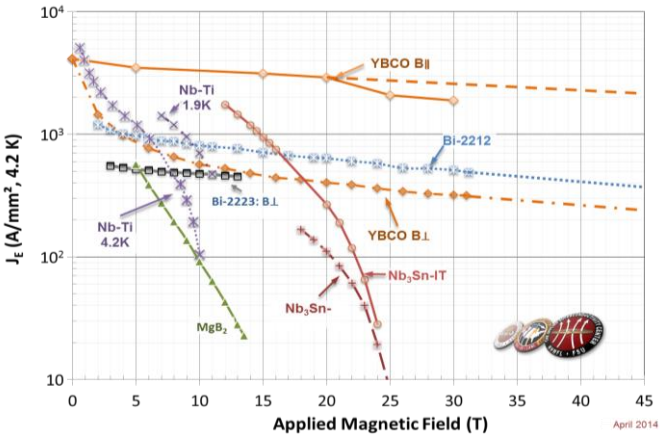

Fig. 4. Engineering current density J_E vs. B for some technical superconductors. Courtesy of P.J. Lee, ASC-NHMFL, USA.

SC wires designed for high-field accelerator magnets have to meet stringent requirements. The HEP community is leading the development of Nb_3Sn wires for post-LHC accelerators since the late 1990s. In 1999, the US Department of Energy began the Conductor Development Program (CDP), a collaborative effort between industry, national laboratories, and universities, with the goal of increasing the J_c value of Nb_3Sn IT wires. As a result of this program, multifilament wires produced using the restack rod process (RRP) by Oxford Superconducting Technology (OST) demonstrated J_c values above 3 kA/mm^2 at 12 T and 4.2 K. In parallel, the CDP optimized J_c, the copper-matrix residual resistivity ratio (RRR), and the effective filament diameter D_{eff} in order to develop strands for 10–12 T SC magnets that are stable with respect to so-called flux jumps.

A parallel effort, started in the early 2000s in the European Union, has focused on the development of large-diameter wires

(up to 1.25 mm), with a J_c value of 1.5 kA/mm^2 at 15 T and 4.2 K, produced by two methods: enhanced internal tin (EIT) and PIT. At present this effort, led by CERN, is focusing on PIT wires produced by Bruker EAS.

Nb_3Sn conductors are also being developed in Japan. These efforts focus on the combination of J_c values at 12 T and 4.2 K, high RRR, and low values of D_{eff} by using the distributed tin method. A research program on Nb_3Al wires based on the RHQT process for accelerator magnets is in progress at KEK and National Institute for Material Science (NIMS).

After the successful industrialization of composite HTSs, the HEP community began monitoring and supporting their development. The US Department of Energy promoted the development of Bi-2212 composite wires through the CDP and other special programs with the goal of improving their performance to a level acceptable for application in accelerator magnets. An important result of this effort was a substantial improvement in the Bi-2212 wire J_c due to heat treatment under pressure of up to 100 bars [14]. Improvements in REBCO tapes, supported mainly by the power industry, are also being monitored by high-field accelerator magnet programs in the United States, Europe, and Japan.

Further improvement in the J_E values of commercial composite HTSs to ~1 kA/mm^2 (or higher) at 20–25 T and 4.2 K is needed in order for them to be used in accelerator magnets. The J_E value of Nb_3Sn composite wires has to be pushed to 1 kA/mm^2 at fields above 15 T.

B. Cables

Round Nb_3Sn, Nb_3Al, and Bi-2212 strands are compatible with the Rutherford cable design traditionally used for accelerator magnets. To make multistrand cables using REBCO tape, the Roebel design is used. Figure 5 shows examples of these two cables.

Fig. 5. Rutherford and Roebel cables.

Rutherford cable R&D carried out at Lawrence Berkeley National Laboratory (LBNL), FNAL, and recently CERN is focused on the optimization of the cable design and processing to minimize the strand critical current (I_c) degradation due to cabling, improvement of cable stability and quench protection, and reduction of eddy current magnetization. The level of strand I_c degradation has been reduced by optimizing the cable packing factor as well as the cable edge and width deformations. The use of a thin stainless steel-core inside the Nb_3Sn cables greatly reduced the coupling currents by minimizing the interstrand crossover resistance. Several interesting ideas have been tested to increase the cross section of stabilizer in the cable, such as mixing copper strands with Nb_3Sn strands, using a thick copper core, and wrapping the cables with thin copper tape.

IV. Nb_3Sn Magnet R&D

Due to their higher T_c and B_{c2} values, Nb_3Sn magnets had long been considered an alternative to NbTi magnets. In the 1990s, Nb_3Sn magnet technology [15]-[17] encouraged design studies for future accelerators using high-field Nb_3Sn accelerator magnets [18]. In turn, the design studies begun in the United States after the termination of the Superconducting Super Collider (SSC) project boosted the R&D efforts in Nb_3Sn magnets at BNL, FNAL, LBNL, and Texas A&M University (TAMU) [19]. In France, during the construction of the LHC, researchers at CEA Saclay continued a small R&D program on Nb_3Sn magnets to use the LHC main quadrupoles with Nb_3Sn coils as components of the Tesla FF system [20]. Meanwhile, at the University of Twente in the Netherlands, an 88-mm-aperture Nb_3Sn dipole was designed to replace the D1 dipoles in the LHC Interaction Regions (IRs) [21].

A staged VLHC design considered low-field and high-field SC rings in a 233-km-long tunnel [3]. The low-field ring used 2 T magnets to reach a beam energy of 20 TeV, as in the SSC. The nominal field in the high-field ring of 10 T, chosen on the basis of a cost analysis, raised the beam energy to 87.5 TeV. These studies stimulated R&D in Nb_3Sn magnets with a nominal field of ~10 T. The studies involved different coil geometries and magnet designs, as well as both W&R and R&W techniques.

A. Twin-aperture common coil dipole models

The second stage of the VLHC design involved the development of a SR with a vertical beam arrangement. The so-called common-coil design was proposed in order to realize this configuration [22]. In a common-coil dipole, two large "racetrack" coils generate in both apertures opposite-direction magnetic fields. Auxiliary coils placed above and below each aperture are used to ensure a field quality suitable for accelerator magnets. Because of its large coil bending radii, this design is compatible with both the W&R and R&W methods. Three 1-m-long common-coil dipole models were developed and tested in the United States to validate the technology and performance of this design. Table 2 provides the design parameters of these models, and Fig. 6 shows the magnet cross sections.

Table 2. Twin-aperture 1-m long common coil dipole models.

Parameter	RD3c	HFDC01	DCC017
Technology	W&R	R&W	R&W
Bore separation [mm]	220	290	220
Aperture [mm]	35	40	31
Yoke OD [mm]	660	550	534
Strand diameter [mm]	0.8	0.7	0.8
No of strands in cable	31, 26	60	30
B_{des} [T]	10.9	10.0	10.2

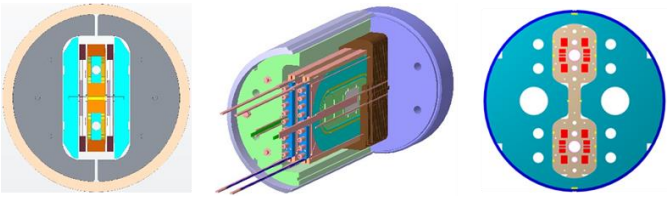

Fig. 6. Twin-aperture common-coil dipole models. (a) RD3c (LBNL), (b) DCC017 (BNL), and (c) HFDC01 (FNAL). Courtesy of R. Hafalia (LBNL), R. Gupta (BNL), and V.V. Kashikhin (FNAL).

A magnet model known as RD3c was developed at LBNL as an inexpensive test of an accelerator-quality common-coil dipole based on the W&R method [23]. The magnet consists of two flat, two-layer racetrack coils on both sides of two apertures and auxiliary coils between the apertures. Prior to their use in RD3c, the outer coils were tested in a simpler configuration, RD3b, without an aperture; they reached the maximum field in the coil of 14.5 T at 4.3 K [24]. The maximum bore field obtained in RD3c after 15 training quenches was 10.03 T at 4.3 K. The measured field harmonics correlated with results from calculations.

A more complicated accelerator-quality common-coil dipole model, HFDC01, was developed and tested at FNAL [25]. This magnet, designed to generate a 10 T field in two 40-mm apertures at 4.5 K, was based on high-performance Nb_3Sn strands and use of the R&W technique. It consists of single-layer coils, a 22-mm-wide 60-strand Rutherford cable, and a stainless-steel collar. Both the left and right coils were wound simultaneously into the collar structure and then filled with epoxy. The R&W method was optimized with a series of simple two-layer racetrack models without an aperture [26]. After a long training period, HFDC01 reached a bore field of only ~6 T and was limited by flux jumps in the superconductor. Results from magnetic measurements confirmed that the good field quality agreed with the magnetic design.

The Nb_3Sn common-coil dipole model DCC017 was made at BNL, also using the R&W technique [27]. This magnet consists of two two-layer flat racetrack coils separated by a clear horizontal space of 31 mm. The mechanical structure includes a stainless-steel collar, a cold yoke, and a stainless-steel skin. The coil ends are supported by thick stainless-steel end plates. After a long training, this magnet reached the expected short sample field of 10.2 T at 4.5 K.

The models described above validated the feasibility and revealed the complexity of the common-coil design. It was recognized that more research is needed to further explore the potential of this design and R&W technology for accelerator magnets, including optimization of the conductor, its structure, and the fabrication process.

B. Single-aperture dipole models

Single-aperture models were used to achieve the highest possible accelerator quality and performance reproducibility of the Nb_3Sn accelerator magnets. R&D efforts at LBNL aimed to demonstrate the Nb_3Sn dipole field limit by using block-type coils [28]. R&D efforts at FNAL focused on demonstrating accelerator-quality magnets based on traditional $cos\theta$ coils [29]. At the same time, the magnet group at TAMU proposed [30] and studied [31] a concept of stress management in high-field dipoles based on block-type coils. Table 3 lists the design parameters of the single-aperture dipole magnets developed and tested at LBNL and FNAL, and Fig. 7 shows the magnet cross sections.

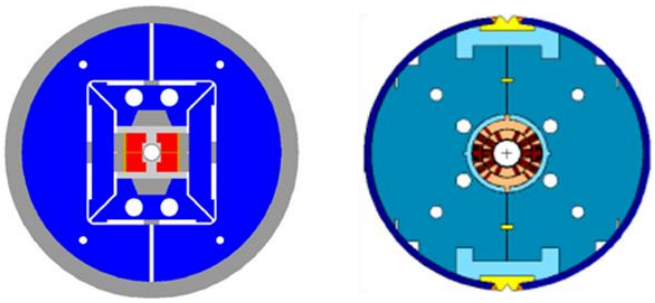

Fig. 7. Single-aperture Nb_3Sn dipole models: (a) HD2/3 (LBNL), (b) HFDA (FNAL). Courtesy of S. Caspi (LBNL) and V.V. Kashikhin (FNAL).

Table 3. Single-aperture 1-m long dipole models

Parameter	**HD2**	**HFDA**
Coil design	Block	Cos-theta
Aperture [mm]	36	43.5
Yoke OD [mm]	625	400
Strand diameter [mm]	0.8	1.0
No of strands in cable	51	27 or 28
B_{max} [T]	15.4	12.2

The first model in the HD series of magnets created at LBNL, HD1, used a flat racetrack coil configuration with only a 10-mm bore [32]. A special support structure based on a thick aluminum shell and a technique involving keys and water-pressurized bladders were used in its construction [33]. HD1 reached a bore field as high as 16 T [34], demonstrating the potential of Nb_3Sn block coils and the coil support structure.

The HD2 and HD3 dipole models of this series were designed to achieve a field above 15 T at 4.3 K and normalized field harmonics below one unit (10^{-4}) in a clear bore of 36 mm [35]. The HD2/3 cross section consists of two two-layer coil modules. A stainless-steel pipe, placed between the top and bottom coils, forms the magnet aperture. To accommodate the pipe in magnet ends, the ends of two midplane racetrack coils are flared. Similar to HD1, the HD2/3 mechanical structure uses a thick aluminum shell and the key-and-bladder preloading technique. The HD2 design peak field in coils is ~16 T. The low-order geometrical field harmonics in aperture are less than 0.1 units at the reference radius R_{ref} of 10 mm. The yoke cross section was optimized to reduce the saturation effects.

Figure 8 shows the bore field versus training quench number for five HD2 model tests at 4.3 K. The HD2c model reached its maximum field in the aperture of 13.8 T (the record dipole field at present!), or 85% of magnet design field [36]. Attempts to improve the conductor insulation and the coil end design in the HD3 model did not improve the magnet performance.

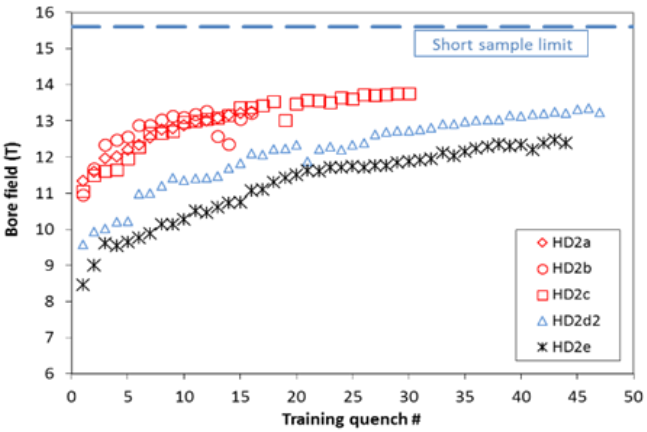

Fig. 8. The HD2 bore field as a function of training quenches. The short sample limit corresponds to a 15.4 T bore field. Courtesy of S. Caspi (LBNL).

The HFDA dipole models at FNAL were designed to deliver a nominal field of 10-11 T in a 43.5-mm bore at 4.5 K [37]. The magnet design consists of a two-layer shell-type coil and a cold iron yoke. The coils are wound using a 14.2-mm-wide, 27-strand Rutherford cable with 1 mm diameter strands. A compact collarless mechanical structure with aluminum clamps, a 400-mm-diameter iron yoke, and a 10-mm-thick stainless-steel skin were used to reduce magnet costs.

Six HFDA short dipole models were fabricated and tested [38]. The HFDA series, the first in the world series of practically identical Nb_3Sn dipoles, provided the first data on the reproducibility of quench performance and field quality in Nb_3Sn accelerator magnets. The first three dipole models were limited by flux jumps in the superconductor and reached only 50–60% of their design field. The last three models, made of more stable 1-mm PIT-192 strands, reached the magnet short sample fields of 9.4 T at 4.5 K and 10.2 at 2.2 K. Figure 9 shows the quench performance of the PIT dipole models. The field level reached in these models was limited by the relatively low J_c value of the PIT strands. A dipole coil made of higher-J_c RRP-108/127 strands and tested in a dipole mirror structure reached a B_{max} value of 11.4 T at 4.5 K.

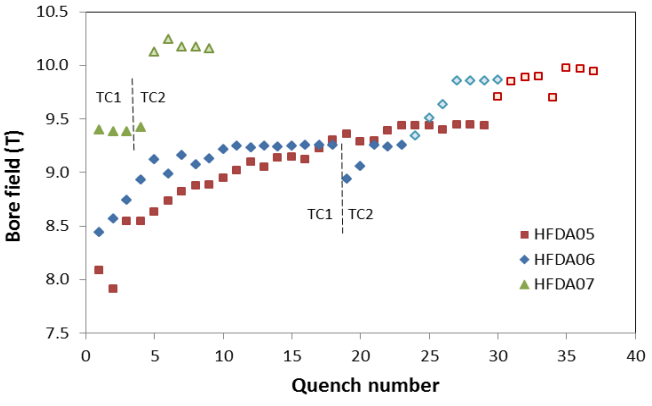

Fig. 9. HFDA model training at 4.5 K (filled symbols) and 2.2 K (open symbols) in thermal cycles TC1 and TC2.

The HFDA-series magnets demonstrated the robustness of both the Nb_3Sn coil technology and the dipoles' mechanical structure. Coil fabrication involved ~20 1-m-long coils, as well as 2-m-long and 4-m-long coils [39]. These efforts also demonstrated the possibilities of (a) a significant reduction in the time needed to fabricate Nb_3Sn magnets and (b) a reduction in cost to a level comparable to that of the NbTi magnets. Fabrication and testing of 2-m-long and 4-m-long coils represented the first time the Nb_3Sn coil technology was scaled up. An efficient passive correction involving the use of iron shims to reduce the effect of large conductor magnetization on field quality at low fields was developed and demonstrated using the HFDA dipole series [40].

C. Large-aperture quadrupole models

Taking into account the larger temperature margin, researchers considered using Nb_3Sn magnets for a new generation of FF quadrupoles for the high-luminosity LHC (HL-LHC) experiments [41], [42]. In 2003, the US Department of Energy launched an R&D program named the LHC Accelerator Research Program (LARP). Magnet research groups from three US national laboratories (BNL, FNAL, and LBNL) collaborated in developing large-aperture high-field Nb_3Sn quadrupoles for the future LHC luminosity upgrade [43]. Figure 10 shows the quadrupole models built and tested by LARP, and Table 4 shows the magnet design parameters.

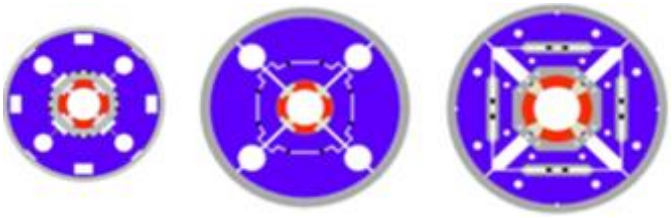

Fig. 10. LARP Nb_3Sn quadrupole models: TQC (left), TQS (center), HQ (right). Courtesy of P. Ferracin (CERN).

Table 4. Quadrupole model design parameters.

Parameter	TQC	TQS	HQ
Aperture [mm]	90	90	120
Yoke OD [mm]	400	556	520
Strand diameter [mm]	0.7	0.7	0.8
No of strands in cable	27	27	35
G_{max} [T/m]	233	239	219
B_{max} [T]	12.1	12.2	15.2

The LARP quadrupole models addressed various aspects of the Nb_3Sn quadrupole technology, including the shell-type coil design, mechanical structures based on an external aluminum shell preloaded with water-pressurized bladders (TQS series) [44], the collar-based structure with two collar types and collaring techniques (TQC series) [45], the Nb_3Sn quadrupole length scale-up (LQS series) [46], and the large aperture and accelerator quality (HQ series) [47]. The LARP quadrupole models were also used to test new Nb_3Sn strands and to study quench performance, field quality, and quadrupole quench protection issues.

All the quadrupole coils use a two-layer coil design, without interlayer splice, and Rutherford cables. The coil fabrication process is based on the W&R technique. LARP Nb_3Sn coil

production involves ~35 TQ-series coils; ~20 HQ-series coils; and 14 4-m-long, 90-mm quadrupole coils and one 4-m-long, 120-mm quadrupole coil fabricated at BNL, FNAL, and LBNL using a distributed production process. The coil technology developed at FNAL and used by the LARP demonstrated good reproducibility of the major coil parameters and a short fabrication time. The robustness of these technologies was confirmed by the success of the distributed fabrication process, the handling and transportation of the short and long Nb_3Sn coils across the United States and to Europe, and multiple coil reassemblies with different mechanical structures that led to no performance degradation.

More than 20 1–1.5-m-long quadrupole models of the TQC, TQS, and HQ series, as well as 4 4-m-long LQS quadrupoles [48]-[52], were fabricated and tested, expanding and enriching the results and our understanding of Nb_3Sn accelerator magnets. Figure 11 shows the training data for representative TQC, TQS, and LQS quadrupoles. Both short and long models reached the design goal of 200 T/m for the field gradient, even at a temperature of 4.5 K. The maximum field in some short and long quadrupole coils exceeded 13 T at 1.9 K. The advances in Nb_3Sn accelerator magnet technology during the past decade have made it possible for the first time to consider Nb_3Sn magnets with nominal fields of up to 12 T (B_{max} values of up to 14–15 T) in present and future machines.

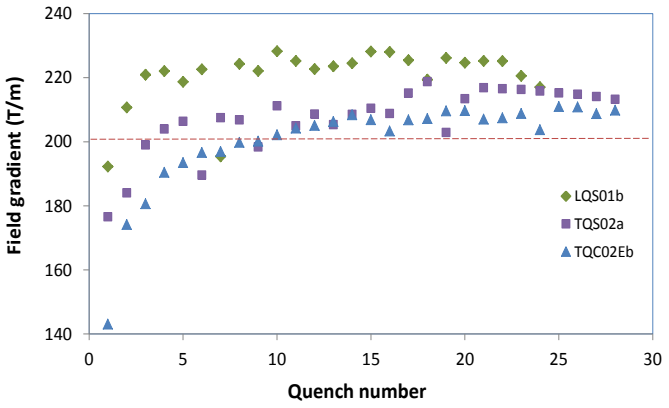

Fig. 11. Field gradient versus quench number at 4.5 K for short models, TQC and TQS, and for a 4-m-long model, LQS.

V. Nb_3Sn Magnets for HL-LHC

LHC is the first accelerator that requires Nb3Sn magnets. Beginning in 2015, after the machine upgrade during the first long shutdown (LS1), the LHC will deliver ~300 fb^{-1} of integrated luminosity at 13–14 TeV center-of-mass energy to both the CMS and ATLAS experiments by 2022. After that, the time needed to reduce statistical errors and perform rare physics searches will become unacceptably long. Therefore, a plan for a luminosity upgrade, called HL-LHC, to collect ~3,000 fb^{-1} per experiment in the following 10 years has been proposed [53]. In order to reach this goal, some dipole magnets in the dispersion suppression (DS) area and low-β quadrupoles in high-luminosity IRs will require a substantial upgrade using the Nb_3Sn technology. Figure 12 depicts the cross sections of these magnets (11 T DS dipoles and MQXF IR quadrupoles), and Table 5 summarizes the magnet parameters.

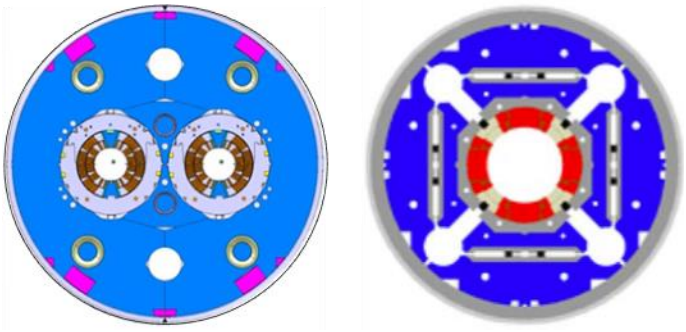

Fig. 12. Cross-sections of the 11 T DS dipole (left) and the 150 mm QXF quadrupole (right). Courtesy of F. Savary and P. Ferracin (CERN).

Table 5. MQXF and 11T Dipole main parameters

Parameter	11T dipole	MQXF
Coil aperture	60 mm	150 mm
Nominal field or gradient	11.2 T	140 T/m
Nominal current I_{nom}	11.85 kA	17.5 kA
Coil peak field at I_{nom}	11.6 T	12.1 T
Margin along the load	19%	20%
Stored energy at I_{nom}	0.97 MJ/m	1.3 MJ/m

A. *11 T DS dipole*

Additional collimators will be placed in the DS areas around points 2, 3, and 7 as well as around ATLAS and CMS detectors in points 1 and 5 [54]. Creating a space for these collimators requires replacing several 15-m-long, 8.33 T NbTi main (MB) dipoles with shorter, 11 T Nb_3Sn (MBH) dipoles. These dipoles have to be compatible with the LHC lattice and main systems and will deliver the same integrated strength at the LHC nominal operation current of 11.85 kA. To validate this approach, researchers at CERN and FNAL are jointly developing a 5.5-m-long, 11-T, twin-aperture Nb_3Sn dipole prototype. Two of these magnets, with a collimator between them, will replace one MB dipole. Another important goal of the program has been the Nb_3Sn technology transfer from FNAL to CERN.

Design concepts of the 11 T Nb_3Sn dipole in both single-aperture and twin-aperture configurations are described elsewhere [55], [56]. The dipole design features two-layer shell-type Nb_3Sn coils, separate stainless-steel collars for each aperture, and the MB yoke modified in the area of the collar–yoke interface. The magnet coil, made of a Rutherford cable with 40 0.7-mm strands and a 0.025-mm-thick stainless-steel core, was designed to provide a dipole field of 11 T with a 20% margin in a 60-mm aperture at the LHC nominal current of 11.85 kA and temperature of 1.9 K. The 60-mm coil aperture is slightly larger than the MB dipole aperture to avoid bending the Nb_3Sn coils to accommodate the LHC beam sagitta. The use of separate collars for each aperture simplifies magnet assembly and reduces the risk of coil damage during assembly. A 2-m-long single-aperture Nb_3Sn dipole demonstrator was fabricated and tested at FNAL in June 2012 [57]. To improve the magnet design and performance and demonstrate performance

reproducibility, FNAL researchers fabricated seven 1-m-long coils in 2012–2014. Four 1-m-long coils were collared and tested at FNAL, first in a single-aperture configuration. Both collared coils were trained to ~11.6 T at 1.9 K, or 97% of the dipole design field of 12 T. Important information about the magnet quench performance and field quality, including geometrical harmonics, coil magnetization, iron saturation, and dynamic effects in 11 T dipole models, was obtained through these studies. The two tested 1-m-long collared coils were assembled in the first twin-aperture dipole model and successfully tested at FNAL in March 2015 [58] reaching after training the expected field in apertures of 11.5 T at 1.9 K. In 2014, researchers at CERN began fabricating and testing 2-m-long single-aperture 11 T dipole models. Two twin-aperture models will also be assembled and tested in 2015–2016, prior to fabrication and testing of the 5.5-m-long 11 T twin-aperture dipole prototype [59]. Magnet production will take place at CERN in collaboration with industry. The first two cryo-assemblies, each with two 5.5-m-long 11 T dipoles with a collimator between them, will be produced in 2018–2019 for installation around Interaction P2 during the second long shutdown (LS2) in 2019. An additional eight cryo-assemblies are planned for installation in 2023–2024 around ATLAS and CMS detectors, and around P7 during the third long shutdown (LS3).

B. *Large-aperture IR quadrupoles*

In order to substantially increase the peak luminosity of the collider, the new LHC high-luminosity IR optics has to provide reduction of the beam size (β^*) in the IPs, which in turn will lead to a larger beam size and, thus, a larger aperture of the IR quadrupoles. Moreover, strong thick shielding is needed inside the quarupole aperture [60] to limit the radiation damage and heat depositions in magnet coils, which are proportional to the integrated and peak luminosity, respectively.

These considerations led to a quadrupole design with a 150-mm aperture and a nominal field gradient of 140 T/m with a 20% margin along the load line at 1.9 K [61]. Recently, in order to increase the operational margin, the field gradient specification has been modified to a slightly reduced level of 133 T/m. Such quadrupoles, referred as QXF, are being developed by a collaboration between LARP and CERN. This development rests on the strong foundation formed by ~10 years of successful R&D of large-aperture high-field Nb_3Sn quadrupoles in the United States. The nominal operation current of QXF quadrupoles is 16.5 kA. The maximum field in the coil at the nominal current is ~11.5 T.

These magnets use the mechanical structure similar to the structure developed for TQ and HQ quadrupoles. Each magnet contains a Rutherford cable, made of 40 strands 0.85 mm in diameter and incorporating a 12-mm-wide and 0.025-mm-thick stainless-steel core, to reduce eddy current effects. The cable insulation is 150 μm thick and is made of S2 glass fibers braided directly on the cable. Two options are being considered for the basic SC strand: the RRP strand by OST and the PIT design by Bruker EAS.

A small series of 1.5-m-long QXF models are being produced by LARP and by CERN prior to the fabrication of the full-scale prototypes and quadrupole production. The first short models will be fabricated and tested by the LARP Collaboration and CERN in 2015, and the first ~ 4-m-long quadrupole prototypes will be produced by fall 2016. Magnet production will start in 2018 both in the United States and in the Europe and will last 4 years [62].

VI. Magnets for Future Colliders

A. *Nb_3Sn magnets for Muon Collider*

A high-energy high-luminosity MC represents a new class of lepton colliders with great discovery potential. High-field SC dipoles and quadrupoles are used in the MC SR and IRs. The dipole magnets must provide a magnetic field of ~10 T to reduce the ring perimeter and, thus, maximize the number of collisions during the muon lifetime. All the magnets require a Nb_3Sn superconductor to achieve the necessary operating parameters with sufficient margins for reliable machine operation.

SC coils need to be protected from showers produced by electrons from muon decay. The high level and distribution of heat deposition in MC SR require either large-aperture magnets to accommodate thick, tungsten absorbers to shield the coils or an open midplane (OM) design to allow passage of the decay electrons to absorbers placed outside the coils.

Both magnet design concepts have been carefully analyzed [63], [64]. In addition to the issues of a lower operation margin, the difficulty of handling the large vertical forces in coils with midplane gaps, and complicated coil cooling and quench protection, the dynamic heat load in OM dipoles is still large because the transverse momentum of the decay electrons is too high for them to pass through the OM with a strong vertical defocusing field in the gap. Furthermore, for muon beam energies above 1.5 TeV, a dipole component is also needed in the quadrupoles to mitigate the neutrino radiation problem. Achieving the required value of both quadrupole and dipole field components in OM combined-function magnets poses serious design challenges. Thus, the researchers decided in favor of large-aperture magnets. Figure 13 shows the cross sections of 150-mm-aperture arc magnets with shell-type coils selected for a 1.5 × 1.5 TeV MC SR [65].

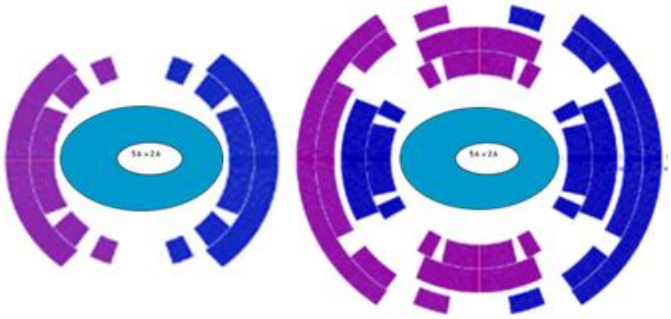

Fig. 13. 150-mm aperture dipole (left) and combined dipole/quadrupole coils (right) with thick internal absorber. Courtesy of V.V. Kashikhin (FNAL).

The MC FF system, based on doublet and triplet layout, was studied in [66] and [67]. Its quadrupole parameters are listed in Table 6. The FF quadrupoles are based on two-layer shell-type coils with apertures ranging from 80 to 180 mm [67].

Table 6. IR Quadrupole Parameters at 4.5 K.

Parameter	Q1	Q2	Q3	Q4-6	Q7	Q8-9
Aperture (mm)	80	100	125	140	160	180
B_{max} coil (T)	14.1	14.3	14.5	14.7	14.8	15.2
G_{max} (T/m)	308	249	202	182	161	127
G_{op} (T/m)	250	200	161	144	125	90
Margin G_{op}/G_{max}	0.81	0.80	0.80	0.79	0.78	0.71
E at G_{op} (MJ/m)	0.7	0.8	1.1	1.2	1.4	1.1

Neutrino radiation is an important factor for a TeV-scale MC. In the quadrupoles nearest to the IP, the natural beam divergence is sufficient to spread this radiation, but in more distant quadrupoles, an additional bending field of ~2 T is necessary. This bending field is created by special dipole coils in quadrupoles Q8 and Q9.

The MC quadrupole parameters are close to those of the LARP quadrupoles described above. However, for MC IR operation at 4.5 K with a proper margin, these magnets require an increase in coil thickness. Focused R&D will be needed for larger-aperture quadrupoles (inner diameter ~180–200 mm) with dipole windings as well as for challenging large-aperture SR dipoles and quadrupoles.

B. Nb_3Sn magnets for Hadron Collider

HCs are considered the most powerful discovery tools in HEP. An interest in an HC with energy beyond the LHC's reach gained additional momentum in the context of recent strategic plans developed in the United States, European Union, and China. To build an ~100 TeV HC in an ~100 km tunnel, ~15 T dipoles operating at 1.9 or 4.5 K with a 15–20% operation margin are needed. The required nominal field of ~15 T enables use of the Nb_3Sn technology. The main challenges for this category of Nb_3Sn magnet include substantially higher electromagnetic forces and higher storage energy. A substantial reduction in the cost of producing the magnets will be key for the practical realization of such a machine. The development and demonstration of cost-effective 15-16 T Nb_3Sn accelerator dipoles have started in the United States, European Union, and Asia and are planned to take place over the next 5–10 years.

The European EuCARD program is exploring the block-type dipole design. At present it is developing 100-mm-aperture Nb_3Sn dipole magnet called FRESCA2 to upgrade the cable test facility at CERN [68]. With a target bore field of 13 T, this magnet is designed for a maximum bore field of 16.0 at 4.2 K or 17.2 T at 1.9 K. It incorporates the design concept of LBNL's HD models and consists of four 1.5-m-long double-layer coils wound with a 21-mm-wide cable. The coils are supported by a structure based on a 65-mm-thick aluminum shell and installed using the key-and-bladder preloading technique. The coils of FRESCA2 are wound with a Rutherford cable composed of 40 strands 1 mm in diameter. Fabrication is in progress, and a test is planned for 2016.

FNAL is developing a 15 T Nb_3Sn dipole demonstrator by using four-layer shell-type coils. First, the existing 11 T dipole developed for the LHC upgrade [55] will be modified by adding another two layers to achieve a 15 T field in a 60-mm aperture. Then, the subsequent model will use an optimized four-layer graded coil. The magnet and tooling design is in progress, and a test of the first model is planned for 2016.

LBNL is working on the canted cosine theta (CCT) dipole design to achieve a significant reduction in conductor stress [69]. Figure 14 shows the tilted solenoid windings, each supported by a channel. Several tests, each with larger number of coil layers and higher fields, are planned for 2015–2016. The tests will begin with 2 layers that yield a 10 T field in a 90-mm bore; later, 6 extra layers will gradually raise the field to 16 T.

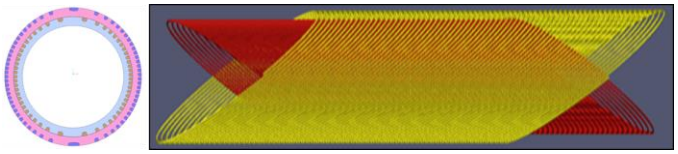

Fig. 14. A canted *cosθ* dipole coil. Courtesy of S. Caspi (LBNL).

A high-field accelerator magnet R&D program has recently been launched in China (https://indico.cern.ch/event/328599/session/4/contribution/20/material/slides/1.pdf). During 2015–2020, the program will develop a twin-aperture Nb_3Sn dipole based on the common-coil configuration with a nominal operation field of 12 T and accelerator field quality. In 2020–2025, the program will develop a 15 T, twin-aperture, accelerator-quality Nb_3Sn dipole and quadrupole.

In Japan, KEK has been developing a subscale magnet [70] to demonstrate the feasibility of Nb_3Al cables, carrying out R&D on relevant magnet technologies such as insulation, and performing a radiation resistance study.

C. HTS magnets

The Nb_3Sn magnet technology is ultimately limited by the B_{c2} values of Nb_3Sn superconductors (~27 T) and the conductors' ability to transport current at high fields. For Nb_3Sn dipoles, the ultimate nominal field is limited by 15–16 T. A breakthrough in high-field pinning in Nb_3Sn may result in an increase of the achievable field to perhaps 20 T [71]. However, to surpass these fields, the magnets need HTS materials which have much higher B_{c2} values.

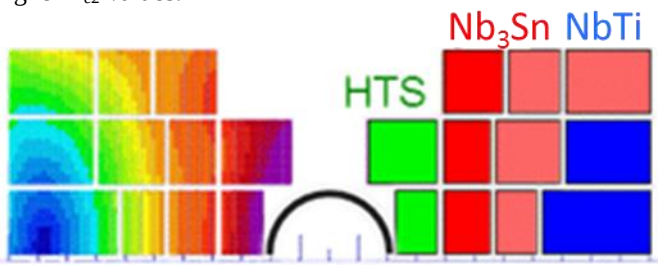

Fig. 15. Hybrid coil with high- and low-temperature superconductors. Courtesy of E. Todesco (CERN).

Fig. 16. High-temperature superconductor inserts inside low-temperature superconductor background magnet based on (a) block and (b) *cosθ* coils. Courtesy of G. de Rijk (CERN) and C. Lorin (CEA Saclay).

Figures 15 and 16 depict the two main approaches to the HTS accelerator magnets presently under consideration. The first approach uses hybrid coils made of HTSs and LTSs [72]. The second approach uses HTS inserts placed inside LTS magnets [73], [74]. In both cases, superconductor grading is used to reduce magnet cost and make the best use of the materials' properties. To save volume and cost, the LTS part of the coil is further divided into Nb_3Sn and NbTi subsections.

The HTS/LTS coil shown in Fig. 15 uses the block design chosen on the basis of a simpler separation between the HTS and LTS regions as well as stress considerations. This coil design relies on flared ends, which require conductor bending in the "hard" direction; thus, the design needs experimental validation, especially for HTS tapes.

The HTS inserts shown in Fig. 16 are based on both block (Fig. 16a) and shell-type (Fig. 16b) coils. HTS inserts based on CCT design are also being developed [75]. The inserts need their own mechanical structure, which should be compatible with the HTS coil design and technology and with the outsert magnet.

The use of HTS coils poses serious challenges for accelerator magnets due to the specific properties of HTSs and the use of HTS coils to date has been limited. The main issues to be addressed for both HTS/LTS hybrid coils and HTS inserts include a substantial increase of the J_E value of the HTS in order to reach operation fields of 5–7 T with a sufficient margin and optimal coil volume; development of high-current HTS cables to reduce HTS coil inductance and, thus, simplify their quench protection; development of robust fabrication technology for HTS coils; stress management in coils; coil/insert integration with LTS coils/magnets; and quench detection and HTS coil protection.

The primary candidate HTS materials are REBCO (in particular, YBCO) tapes and Bi-2212 round wires. The properties of these materials are discussed in Section 3. HTS magnet programs for accelerator magnet are under way in the United States, European Union, and Asia. The development of HTS materials and technologies for high-field accelerator magnets is taking place at national laboratories and universities, which have the necessary infrastructure. These activities are also supported by the conductor industry.

Researchers at BNL have actively pursued magnet technology based on REBCO tapes and a racetrack configuration that is amenable to the common-coil implementation, although they have also considered cosine-theta designs [76]. The BNL YBCO technology is currently being implemented by the FRIB project [77]. The magnet group at LBNL has focused primarily on Bi-2212 cable and coil technology development. Recently, significant effort was made at LBNL in material compatibility studies and in development of the W&R process using Bi-2212 in a racetrack configuration [78], as well as in quench modeling for magnet protection [79]. These HTS efforts are now focused on CCT Bi-2212 inserts [75]. FNAL researchers have investigated the use of REBCO tapes for high-field solenoids for an MC cooling channel [80], [81]. In parallel, they are studying Bi-2212 and YBCO cables [82], [83] and working with other groups in the United States to optimize the heat treatment process for accelerator magnet applications.

The Applied Superconductivity Center of the National High Magnetic Field Laboratory (NHMFL) has invested in understanding and improving YBCO and Bi-2212 materials, motivated by their need for high-field solenoids, high-field accelerator magnets, and other applications [84]. Recent research on overpressure processing of Bi-2212 wires has resulted in a doubling of the J_c value at high fields, making the material competitive with Nb_3Sn at 16 T [14]. The research program at North Carolina State University is addressing issues ranging from HTS material characterization to HTS magnet diagnostic development, including investigation of magnet protection issues [85]. TAMU has invested in stress management concepts for Nb_3Sn magnets and is now pursuing these concepts with HTS inserts as well [86].

The European program EuCARD2 [87] is considering YBCO as its primary option, complementing the US's commitment to develop Bi-2212 technology. YBCO coil technology is also being pursued at CERN for high-field inserts [73], [74], [88]. Magnetic layouts of graded YBCO, Nb_3Sn, and NbTi coils based on the block design have been developed, and conceptual studies of the coil stresses have been initiated. Design studies of hybrid systems with HTS coils have also been initiated at CEA Saclay [89].

HTS and magnet R&D programs are also advancing in Asia. In 2014, Kyoto University hosted a workshop on high-field HTS development for accelerator magnets (https://indico.cern.ch/event/319762/). In China, 15 T Nb_3Sn coils will be combined with HTS coils to produce 20 T dipole and quadrupole prototypes for SppC (https://indico.cern.ch/event/328599/session/4/contribution/20/material/slides/1.pdf).

VII. Summary

Advances in Nb_3Sn accelerator magnet technology during the past decade have made it possible to consider using this technology in present and future machines. The LHC is the first accelerator that will use 60-mm-aperture 11 T Nb_3Sn dipoles and 150-mm-aperture low-β quadrupoles to reach ~3,000 fb^{-1} per experiment within the 10 years of operation. These magnets are planned to be installed in 2018–2019 during LS2 and in 2023 during LS3. 10 T Nb_3Sn magnets with a large margin (B_{des}~14–15 T) are also needed in MC SR and IRs. The Nb_3Sn magnets with nominal operation fields of up to 15-16 T will be also needed for the FCC. Research on the development and demonstration of cost-effective 15-16 T Nb_3Sn accelerator dipoles is under way in the United States, the European Union, and Asia and is planned to continue for the next 5–10 years.

Recent progress in HTS strands and cables is enabling access to magnetic fields of 20 T and beyond. The development and demonstration of this field level using HTS magnets are at the early stage. Realistic insert magnets generating self-fields of 4–5 T are likely to be built within the next few years. However, implementation in a significant background field will likely require a number of additional steps.

An important step toward creating a 20 T dipole with HTS insert coils is the development of a large-aperture (~150–200 mm), 15 T Nb_3Sn dipole with stress management. Such a dipole would deliver a ~15 T background field for the HTS inserts, providing a substantial reduction in the total cost of 20 T

magnets. This magnet would also demonstrate the feasibility of large-aperture high-field magnets for MC and accelerator interaction regions.

Acknowledgment

The writing of this review was supported by Fermi Research Alliance, LLC, under contract DE-AC02-07CH11359 with the US Department of Energy and by the Director, Office of Science, High Energy Physics, U.S. Department of Energy under contract DE-AC02-05CH11231.

References

[1] Abe F, et al. Phys. Rev. Lett. 74:2426 (1994); Abachi S, et al. Phys. Rev. Lett. 74:2632 (1994)
[2] ATLAS Collab. Phys. Lett. B 716:1 (2012); CMS Collab. Phys. Lett. B 716:30 (2012)
[3] Limon P, et al. Design study for a staged Very Large Hadron Collider. Report Fermilab-TM-2149, Fermi Natl. Accel. Lab., Batavia, IL. http://lss.fnal.gov/archive/test-tm/2000/fermilab-tm-2149.pdf (2001)
[4] Geer S. Annu. Rev. Nucl. Part. Sci. 59:347 (2009)
[5] Jackson JD, Panofsky WKH. Edwin Mattison McMillan 1907–1991: A Biographical Memoir. Washington, DC: Natl. Acad. Sci. http://www.nasonline.org/publications/biographical-memoirs/memoir-pdfs/mcmillan-edwin.pdf (1996); Veksler VI. C. R. Acad. Sci. 43:329 (1944)
[6] Mohl D, Petrucci G, Thorndahl L, van der Meer S. Phys. Rep. 58:76 (1980)
[7] Edward HT. Annu. Rev. Nucl. Part. Sci. 35:605 (1985)
[8] Wolff S. IEEE Trans. Magn. 24:719 (1988)
[9] Anerella M, et al. Nucl. Instrum. Methods A 499:280 (2003)
[10] Rossi L. IEEE Trans. Appl. Supercond. 13:1221 (2003)
[11] Bottura L, Godeke A. Rev. Accel. Sci. Technol. 5:25 (2012)
[12] Tsuchiya K, et al. IEEE Trans. Appl. Supercond. 14:1016 (2004)
[13] Kumakura H. Jpn. J. Appl. Phys. 51:010003 (2012)
[14] Jiang J, et al. Supercond. Sci. Technol. 24:082001 (2011)
[15] Asner A, Perin R, Wenger S, Zerobin F. In Proceedings of the 11th International Conference on Magnet Technology, ed. T Sekiguchi, S Shimamoto, p. 36. Amsterdam: Springer (1990)
[16] den Ouden A, et al. IEEE Trans. Appl. Supercond. 7:733 (1997)
[17] McInturff AD, et al. In Proceedings of the 1997 Particle Accelerator Conference, ed. M Comyn, MK Craddock, M Reiser, J Thomson, p. 3212. Piscataway, NJ: IEEE (1997)
[18] New directions for High-Energy Physics. Proc. of the 1996 DPF/DPB Summer Study on High-Energy Physics, June 25-July 12, Snowmass, Colorado (1996), editors D.G. Cassel, L. Trindle Gennari, R.H. Siemann
[19] Gourlay SA. IEEE Trans. Appl. Supercond. 14:333 (2004)
[20] Devred A, et al. Development of a Nb3Sn quadrupole magnet model. Report DAPNIA/STCM-00-23, CEA Saclay, Gif-sur-Yvette, France (2000)
[21] den Ouden A, et al. IEEE Trans. Appl. Supercond. 11:2268 (2001)
[22] Gupta RC. In Proceedings of the 1997 Particle Accelerator Conference, ed. M Comyn, MK Craddock, M Reiser, J Thomson, 3:3345. Piscataway, NJ: IEEE (1997)
[23] Liedzke AF, et al. IEEE Trans. Appl. Supercond. 13:1292 (2003)
[24] Benjegerdes R, et al. In Proceedings of the 2001 Particle Accelerator Conference, Chicago (IL), p. 208 (2001)
[25] Kashikhin VS, et al. IEEE Trans. Appl. Supercond. 14:353 (2004)
[26] Ambrosio G, et al. IEEE Trans. Appl. Supercond. 13:1284 (2003)
[27] Gupta R, et al. IEEE Trans. Appl. Supercond. 17:1130 (2007)
[28] Gourlay SA, Sabbi G. In Proceedings of the 8th European Particle Accelerator Conference (EPAC 2002), ed. J-L Laclare, p. 2397. Geneva: CERN (2002)
[29] Zlobin AV, et al. IEEE Trans. Appl. Supercond. 15:1113 (2005)
[30] Elliott T, et al. IEEE Trans. Appl. Supercond. 7:555 (1997)
[31] McInturff, et al. IEEE Trans. Appl. Supercond. 17:1157 (2007)
[32] Hafalia R, et al. IEEE Trans. Appl. Supercond. 14:283 (2004)
[33] Caspi S, et al. IEEE Trans. Appl. Superconduct. 11:2272 (2001)
[34] Lietzke F, et al. IEEE Trans. Appl. Supercond. 14:345 (2004)
[35] Sabbi G, et al. IEEE Trans. Appl. Superconduct. 15:1128 (2005)
[36] Ferracin P, et al. IEEE Trans. Appl. Supercond. 19:1240 (2009)
[37] Ambrosio G, et al. IEEE Trans. Appl. Supercond. 10:298 (2000)
[38] Zlobin AV, et al. In Proceedings of the 2007 Particle Accelerator Conference, p. 482. Piscataway, NJ: IEEE (2007)
[39] Zlobin AV. arXiv:1108.1869 [physics] (2011)
[40] Kashikhin VV, et al. IEEE Trans. Appl. Supercond. 13:1270 (2003)
[41] Sen T, Strait J, Zlobin AV. In Proceedings of the 2001 Particle Accelerator Conference, ed. P Lucas, S Webber, p. 3421. Piscataway, NJ: IEEE (2001)
[42] Ruggiero F, et al, LHC Project Report 626, December 2002
[43] Gourlay SA, et al. IEEE Trans. Appl. Supercond. 16:324 (2006)
[44] Caspi S, et al. IEEE Trans. Appl. Supercond. 16:358 (2006)
[45] Bossert RC, et al. IEEE Trans. Appl. Supercond. 16:370 (2006)
[46] Ambrosio G, et al. IEEE Trans. Appl. Supercond. 18:268 (2008)
[47] Felice H, et al. IEEE Trans. Appl. Supercond. 18:281 (2008)
[48] Bossert RC, et al. IEEE Trans. Appl. Supercond. 19:1226 (2009)
[49] Caspi S, et al. IEEE Trans. Appl. Supercond. 19:1221 (2009)
[50] Bajas H, et al. IEEE Trans. Appl. Supercond. 25:4003306 (2015)
[51] Ambrosio G, et al. IEEE Trans. Appl. Supercond. 22:4003804 (2012)

[52] Sabbi GL. arXiv:1108.1869 [physics] (2011)
[53] Rossi L, Bruning O. CERN ATS 2012-236, 23 (2012)
[54] Bottura L, et al. IEEE Trans. Appl. Supercond. 22:4002008 (2012)
[55] Zlobin AV, et al. In Proceedings of the 2011 Particle Accelerator Conference, p. 1460. Piscataway, NJ: IEEE (2011)
[56] Karppinen M, et al. IEEE Trans. Appl. Supercond. 22:4901504 (2012)
[57] Zlobin AV, et al. IEEE Trans. Appl. Supercond. 23:4000904 (2013)
[58] Zlobin AV, et al. IEEE Trans. Appl. Supercond. 25:4002209 (2015)
[59] Savary F, et al. IEEE Trans. Appl. Supercond. 25:4003205 (2015)
[60] Esposito L, et al. In Proceedings of the 4th International Particle Accelerator Conference (IPAC2013), ed. Z Dai, C Petit-Jean-Genaz, Schaa VRW, Zhang C, p. 1379. JACoW.org: Jt. Accel. Conf. Website (2013)
[61] Borgnolutti F, et al. IEEE Trans. Appl. Supercond. 24:4000405 (2014)
[62] Apollinari G. In Proceedings of the 5th International Particle Accelerator Conference (IPAC2014), ed. C Petit-Jean-Genaz, G Arduini, P Michel, VRW Schaa, p. 983. JACoW.org: Jt. Accel. Conf. Website (2014)
[63] Zlobin AV, Alexahin Y, Kashikhin V, Mokhov NV. In Proceedings of the International Particle Accelerator Conference (IPAC2010), p. 388. JACoW.org: Jt. Accel. Conf. Website (2010)
[64] Novitski I, et al. IEEE Trans. Appl. Supercond. 21:1825 (2011)
[65] Kashikhin VV, Alexahin Y, Mokhov NV, Zlobin AV. In Proceedings of the 3rd International Particle Accelerator Conference (IPAC2012), p. 3587. JACoW.org: Jt. Accel. Conf. Website (2012)
[66] Alexahin YI, et al. Phys. Rev. Spec. Top. Accel. Beams 14:061001 (2011)
[67] Kashikhin VV, Alexahin Y, Mokhov NV, Zlobin AV. In Proceedings of the 3rd International Particle Accelerator Conference (IPAC2012), p. 3584. JACoW.org: Jt. Accel. Conf. Website (2012)
[68] de Rijk G. The High-Energy Large Hadron Collider, In Proceedings of the EuCARD-AccNet_EuroLumi workshop, editors E. Todesco,F. Zimmermann, Malta, 14-16 October (2010); CERN-2011-003
[69] Caspi S, et al. IEEE Trans. Appl. Supercond. 25:4000205 (2015)
[70] Nakamoto T. The High-Energy Large Hadron Collider, In Proceedings of the EuCARD-AccNet_EuroLumi workshop, editors E. Todesco,F. Zimmermann, Malta, 14-16 October 2010; CERN-2011-003
[71] Godeke A, et al. IEEE Trans. Appl. Supercond. 17:1149 (2007)
[72] Todesco E, et al. IEEE Trans. Appl. Supercond. 24:4004306 (2014)
[73] van Nugteren J, et al. IEEE Trans. Appl. Supercond. 25:4000705 (2015)
[74] Lorin C, et al. IEEE Trans. Appl. Supercond. 25:4000305 (2015)
[75] Godeke A, et al. IEEE Trans. Appl. Supercond. 25: 4002404 (2015)
[76] Gupta R, et al. IEEE Trans. Appl. Supercond. 12:75 (2002)
[77] Gupta R, et al. IEEE Trans. Appl. Supercond. 99:1 (2014)
[78] Godeke A, et al. IEEE Trans. Appl. Supercond. 18:516 (2008)
[79] Arbelaez, et al. IEEE Trans. Appl. Supercond. 21:2787 (2011)
[80] Yu M, et al. In Proceedings of the 2011 Particle Accelerator Conference, p. 1118. Piscataway, NJ: IEEE (2011)
[81] Lombardo V, et al. AIP Conf. Proc. 1434, 1381 (2012); doi: 10.1063/1.4707064
[82] Barzi E, et al. Advances in Cryogenic Engineering, V. 53 (2008)
[83] Lombardo V, et al. IEEE Trans. Appl. Supercond. 21:2331 (2011)
[84] Weijers HW, et al. IEEE Trans. Appl. Supercond. 20:576 (2010)
[85] Schwartz J. arXiv.org, vol. physics.acc-ph. 16-Jan-2014
[86] McIntyre PM, et al. arXiv.org. 08-Aug-2011
[87] de Rijk G. IEEE Trans. Appl. Supercond. 22:4301204 (2012)
[88] Kirby GA, et al. IEEE Trans. Appl. Supercond. 25:4000805 (2015)
[89] Devaux M, et al. IEEE Trans. Appl. Supercond. 22:4203605 (2012)